Biochemistry **2000,** *39,* 14831−14838

Mutations in the CD-Loop Region of the D2 Protein in *Synechocystis* sp. PCC 6803 Modify Charge Recombination Pathways in Photosystem II in Vivo[†]

Dmitrii V. Vavilin* and Wim F. J. Vermaas

Department of Plant Biology and Center for the Study of Early Events in Photosynthesis, Arizona State University, Box 871601, Tempe, Arizona 85287-1601

Received July 19, 2000

ABSTRACT: The lumenal CD-loop region of the D2 protein of photosystem II contains residues that interact with the primary electron donor P680 and the redox active tyrosyl residue Y_D. Photosystem II properties were studied in a number of photoautotrophic mutants of *Synechocystis* sp. PCC 6803, most of which carried combinatorial mutations in residues 164−170, 179−186, or 187−194 of the D2 protein. To facilitate characterization of photosystem II properties in the mutants, the CD-loop mutations were introduced into a photosystem I-less background. According to variable fluorescence decay measurements in DCMU-treated cells, charge recombination of Q_A^- with the donor side was faster in the majority of mutants ($t_{1/2} = 45-140$ ms) than in the control ($t_{1/2} = 180$ ms). However, in one mutant (named C7-3), the decay of Q_A^- was 2 times slower than in the control ($t_{1/2} = 360$ ms). The decay half-time of each mutant correlated with the yield of the Q-band of thermoluminescence (TL) emitted due to $S_2Q_A^-$ charge recombination. The C7-3 mutant had the highest TL intensity, whereas no Q-band was detected in the mutants with fast Q_A^- decay ($t_{1/2} = 45-50$ ms). The correlated changes in the rate of recombination and in TL yield in these strains suggest the existence of a nonradiative pathway of charge recombination between Q_A^- and the donor side. This may involve direct electron transfer from Q_A^- to $P680^+$ in a way not leading to formation of excited chlorophyll. Many mutations in the CD-loop appear to increase the equilibrium $P680^+$ concentration during the lifetime of the $S_2Q_A^-$ state, for example, by making the midpoint potential of the $P680^+/P680$ redox couple more negative. The nonradiative charge recombination pathway involves a low activation energy and is less temperature-dependent than the formation of excited P680 that leads to TL emission. Therefore, during the TL measurements in these mutants, the $S_2Q_A^-$ state can recombine nonradiatively before temperatures are reached at which radiative charge recombination becomes feasible. The results presented here highlight the presence of two charge recombination pathways and the importance of the CD-loop of the D2 protein in determination of the energy gap between the $P680^+S_1$ and $P680S_2$ states.

Photosystem II (PS II)[1] is a multisubunit protein complex in thylakoid membranes of plants and cyanobacteria and catalyzes the light-induced reduction of plastoquinone by water (reviewed in refs *1* and *2*). Light energy absorbed by light-harvesting pigment molecules is transferred to the reaction center and causes charge separation between chlorophyll *a* (Chl *a*) that is part of P680 and the primary electron acceptor, pheophytin (Pheo). The charge separation is stabilized upon electron transfer to the primary electron-accepting plastoquinone Q_A and then via Q_B, another plastoquinone molecule, to the plastoquinone pool. The photooxidized $P680^+$ is reduced by a redox active Y_Z (Tyr161 of the D1 protein), and Y_Z^{ox} in turn oxidizes the Mn-containing oxygen-evolving complex. The release of molecular oxygen from water requires four sequential oxidation steps; the corresponding oxidation states of the oxygen-evolving complex are called S_0-S_4. In dark-adapted PS II, the oxygen-evolving complex is predominantly in the S_1 state.

Besides the major electron transfer carriers that participate in electron transfer from water to the plastoquinone pool, at least four other redox active cofactors in PS II can be oxidized by $P680^+$ under certain conditions. These are the redox active tyrosine, Y_D (Tyr160 of the D2 protein), a Chl named Chl_Z, a carotenoid, and cytochrome b_{559} (cyt b_{559}). Y_D, the carotenoid, and Chl_Z are oxidized directly by $P680^+$ (*3*−*5*), whereas oxidation of cyt b_{559} is likely to occur through Chl_Z^+ (*6*). Cyt b_{559} can also act as an electron acceptor in PS II (*7*−*9*), thus creating a pathway of cyclic electron flow around PS II (*9*, *10*). However, the physiological relevance of this putative cycle is still unclear. Recombination of

---

[†] This research was supported by a grant from the National Institutes of Health to W.F.J.V. (GM 51556).

* Corresponding author. Telephone: (480) 965-3698. Fax: (480) 965-6899. E-mail: vavilin@imap4.asu.edu.

[1] Abbreviations: Chl, chlorophyll; cyt, cytochrome; DCBQ, 2,5-dichloro-1,4-benzoquinone; DCMU, 3-(3,4-dichlorophenyl)-1,1-dimethylurea; EPR, electron paramagnetic resonance; F_M, maximal fluorescence; F_O, constant fluorescence; F_V, variable fluorescence; Pheo, pheophytin; PS I, photosystem I; PS II, photosystem II; P680, primary electron donor in PS II; Q_A, primary electron-accepting quinone in PS II; Q_B, secondary electron-accepting quinone in PS II; TL, thermoluminescence; T_M, temperature of maximum thermoluminescence emission; Y_D, tyrosine$_D$ (Tyr160 of the D2 protein), an accessory electron donor in PS II; Y_Z, tyrosine$_Z$ (Tyr161 of the D1 protein), the immediate electron donor to P680.

10.1021/bi001679m CCC: $19.00

charges at the donor and acceptor sides via reverse electron flow may result in the re-creation of the P680* excited state. Another charge recombination mechanism that does not lead to formation of P680* and that may be analogous to the recombination mechanism in purple bacteria (*11*) has been proposed as well (*12*).

When charge recombination occurs by processes leading to the re-formation of excited P680, light emission (delayed luminescence) will be observed (*13*). At low temperatures, charged intermediates can be stabilized and their recombination prevented. Activation of the back reactions in PS II by warming the samples leads to light emission called thermoluminescence (TL) (reviewed in ref *14*).

The smallest unit in PS II that exhibits photochemical activity (formation of the $P680^{+}Pheo^{-}$ state) consists of the D1/D2 heterodimer and small subunits, including cyt b_{559}. The D2 protein consists of five transmembrane helices, and together with D1, this protein binds the cofactors that are crucial for PS II photochemistry. Helices C and D are connected at the lumenal side by the CD-loop (residues 164−195), part of which is presumed to have an α-helical structure. The CD-loop appears to play a key role in determining the structural environment around Y_D, P680, and accessory Chl molecules. One of the residues in this loop, His189, can accept a proton from Y_D when this residue is oxidized (*15*). Arg180 seems to be closely associated with Y_D and Chls that contribute to the properties of P680 (*16*). On the basis of homology-based structural modeling, Phe179 was proposed to provide ring stacking forces to one of the accessory chlorophyll molecules (*17*). Nevertheless, in the absence of a high-resolution X-ray crystal structure of the PS II reaction center, detailed structural information about this complex is still limited.

To evaluate the structural requirements for the function of redox active components at the donor side of PS II, we have employed a combinatorial mutagenesis approach to determine the amino acid combinations in the CD-loop region of the D2 protein that support stable PS II function and photoautotrophic growth. Using this approach, a large number of combinatorial D2 mutants have been generated and the mutations have been introduced into a PS I-less background to facilitate screening of PS II fluorescence characteristics of the mutants (*18*, *19*). As will be presented here, analysis of the properties of mutants and the wild type has provided interesting insights regarding pathways of charge recombination in PS II.

MATERIALS AND METHODS

Growth Conditions. PS I-containing strains of *Synechocystis* sp. PCC 6803 were grown in liquid BG-11 medium (*20*) at 28 °C and 40 $\mu E\ m^{-2}\ s^{-1}$. The rate of growth of the strains was followed by monitoring the optical density at 730 nm using a Shimadzu UV-160 spectrophotometer. The PS I-less mutants were grown at 28 °C and 4 $\mu E\ m^{-2}\ s^{-1}$ in a modified liquid BG-11 medium supplemented with 10 mM glucose and 10 mM TES buffer (pH 8.2). In the modified BG-11 medium, sodium nitrate was replaced with a combination of 1.12 g/L sodium nitrate and 0.35 g/L ammonium nitrate. Cultures were propagated on a rotary shaker (volumes of less than 1 L) or bubbled with air (for larger volumes).

Solid BG-11 medium (standard or modified) used for segregation and maintenance of the mutants was supplemented with 1.5% (w/v) agar, 0.3% (w/v) sodium thiosulfate, and 10 mM TES/NaOH buffer (pH 8.2). Moreover, 10 mM glucose and appropriate antibiotics were added, if required.

Construction of the Mutants. The combinatorial mutants were constructed as described in refs *18* and *19*. The substitution mutants S6 and S8 were obtained by transformation of the D2ΔCD strain, which lacked *psb*DII and the *psb*DI region encoding the CD-loop of D2 (residues Gly163−Pro195) and which carried a kanamycin resistance cartridge downstream of *psb*DIC, with an M13 clone that contained a modified *Synechocystis* sp. PCC 6803 *psb*DI gene. In the S6 strain, codons 171−178 of the *psb*DI gene were replaced with the corresponding codons (172−179) from the *psb*AII gene, which encodes the D1 protein of PS II; in S8, *psb*DI codons 187−194 were replaced with *psb*AII codons 188−195. The resulting transformants were selected for photoautotrophic growth.

Site-directed mutations were introduced into the D2 protein of *Synechocystis* sp. PCC 6803 by transformation of the D2ΔCD strain with M13 clones carrying the desired mutation in *psb*DI (*21*). Transformants were selected for photoautotrophic growth.

To allow a more detailed characterization of selected combinatorial, replacement, and site-directed photoautotrophic mutants, genomic DNA was isolated and used for transformation of the PS I-less *psa*AB^{-}/*psb*DIC^{-}/*psb*DII^{-} *Synechocystis* sp. PCC 6803 strain (*22*) followed by selection for kanamycin resistance (a kanamycin resistance marker linked to *psb*DI was present in the D2ΔCD strain and the photoautotrophic mutants). Kanamycin-resistant transformants in most cases did not incorporate the *psa*AB operon present in the transforming DNA. These transformants were distinguished by the typical blue-green color of colonies lacking PS I, and were selected for use in further experiments.

Chlorophyll Fluorescence Measurements. Chlorophyll fluorescence induction and decay were detected with a PAM fluorometer (Walz, Effeltrich, Germany) and recorded and analyzed using FIP fluorescence software and an ADC-12 card (Q_A-Data, Turku, Finland). To measure the intensities of initial (F_O), maximal (F_M), and variable ($F_V = F_M - F_O$) fluorescence, a cell suspension containing ∼1 μg of Chl/mL was placed in a Walz cuvette, incubated for 3 min in darkness in the presence of 10 μM 3-(3,4-dichlorophenyl)-1,1-dimethylurea (DCMU), and then illuminated for up to 5 s with red monitoring light. The fluorescence signal detected 2−4 ms after turning on the monitoring light was taken to be the F_O value, and the maximum fluorescence signal reached during the illumination period was taken to be F_M.

Decay of variable fluorescence was assessed as follows. After illumination of the sample for 100 ms with red light emitted by a PAM LED lamp (light intensity, 30 $\mu E\ m^{-2}\ s^{-1}$), the actinic light was turned off and the fluorescence yield elicited by weak measuring flashes was recorded. Every trace was recorded using a fresh sample. The measurements were repeated four to six times with each mutant, and the averaged curve was used for further analysis of decay components.

The decay of variable fluorescence in the absence of DCMU (and thereby allowing Q_A to Q_B electron transfer) was recorded after illuminating the sample with a single-turnover Xe flash.

Oxygen Evolution. Oxygen evolution of intact cells under continuous saturating light was assessed in samples taken from liquid cultures (Chl concentration, 0.8−1.5 μg/mL) using a Clark-type electrode at 25 °C in the presence of 1 mM potassium ferricyanide and 0.2 mM 2,5-dichloro-1,4-benzoquinone (DCBQ). Light from a Xe arc lamp was filtered through water and subsequently passed through an orange cutoff filter, transmitting light with a wavelength above 580 nm. The incident light intensity was ~4000 μE m^{-2} s^{-1}. Oxygen evolution in single-turnover flashes was assessed at 20 °C using a Joliot-type oxygen electrode essentially as described in ref *23*.

Thermoluminescence. TL was measured with a home-built apparatus described in ref *24*. Cyanobacteria were concentrated by centrifugation and then resuspended in BG-11 medium to a final concentration of 11−16 μg of Chl/mL. DCMU (50 μM) and glycerol (7%, v/v) were added to the cells just before placing them into the cuvette. The sample was then dark adapted for 5 min and cooled to −40 °C. A sequence of 10 single-turnover flashes was fired at a frequency of 0.5 Hz when the temperature in the cuvette reached −40 °C (multiple flashes were applied to ensure a $S_1Q_A \rightarrow S_2Q_A^-$ transition in essentially all functional PS II centers). The TL signal was recorded upon heating the sample at a rate of 0.4 °C/s.

EPR Measurements. To study the properties of Y_D^{ox}, thylakoid membranes were prepared from different PS I-less strains as described in ref *16*. EPR tubes were filled with ~0.2 mL of the thylakoid suspension (Chl concentration, 200−270 μg/mL), incubated for 2 min at high light intensity (400−600 μE m^{-2} s^{-1}) at room temperature, and then frozen in darkness and stored in liquid nitrogen in the dark. X-band EPR spectra were recorded at 120 K with a Bruker ESP 550E spectrometer. EPR conditions were as follows: microwave power, 1 mW; microwave frequency, 9.41 GHz; modulation amplitude, 0.3 mT; and modulation frequency, 100 kHz.

RESULTS

Photosynthetic Characteristics of the Mutants. Mutants with combinatorial sequences at residues 164−170, 179−186, and 187−194 of the D2 protein were generated by transformation of the D2ΔCD strain with a mixture of M13 DNA carrying combinatorial sequences of the corresponding codons of *psb*DI (*18*, *19*). Transformants with significant photoautotrophic growth rates were selected, and the mutated region of *psb*DI was sequenced. Several other mutants have been used in this study as well. These include S6, in which residues 171−178 of the D2 protein were substituted with the corresponding sequence of the D1 protein (codons 172−179 of *psb*AII), S8, in which residues 187−194 of the D2 were replaced with residues 188−195 of the D1 protein, and three site-directed mutants with single mutations in the D2 protein (F188E, W191L, and T192A). Their photoautotrophic growth rates in liquid BG-11 medium are listed in Table 1. Subsequently, DNA from all mutants used in this study was introduced into a *psa*AB$^-$/*psb*DIC$^-$/*psb*DII$^-$ strain to generate these mutants in a PS I-less background to facilitate screening of their PS II characteristics.

The maximum rates of oxygen evolution of the PS I-less CD-loop mutants in the presence of 0.2 mM DCBQ were more than 75% of the control value, which was 1900 ± 150 μmol of O_2 (mg of Chl)$^{-1}$ h^{-1} in the PS I-less strain with the wild-type CD-loop sequence. The high rate of oxygen evolution was observed even in strains in which the PS I-containing counterparts had substantially reduced growth rates (for example, mutants C5-1, C5-4, and C5-8) possibly because of reduced amounts of PS II in these PS I-containing mutants. The flash-induced oxygen release pattern at a flash frequency of ≥2.5 Hz generally was similar to that of the control, indicating a normal functioning of the water-splitting complex. The F_V/F_M ratio varied from 0.33 ± 0.04 in the C7-3 mutant to 0.68 ± 0.03 in the control PS I-less strain containing the wild-type CD-loop sequence. The F_V yield in the C7-3 mutant was presumably reduced due to quenching of excitations by Trp181 (*23*). Despite the low F_v yield, the C7-3 mutant exhibited significant photoautotrophic growth in a PS I-containing background (Table 1), and its maximal rate of oxygen evolution measured in the PS I-less cells was close to normal.

Table 1: Mutants Used in This Study and Their Photosynthetic Characteristics[a]

Strain	D2 amino acid sequence (residues 164-194)	Doubling time, % of wild type[b]	F_v decay[c], $t_{1/2}$, ms
WT	QSSWFFA PSFGVAGI FRFILFLQ GFHNWTLN	100	180±10
C5-1	**H**SS**MVT**A PSFGVAGI FRFILFLQ GFHNWTLN	390±60	68± 3
C5-1	Q**G**S**MA**F**G** PSFGVAGI FRFILFLQ GFHNWTLN	105±11	142±14
C5-4	Q**A**S**NL**F**G** PSFGVAGI FRFILFLQ GFHNWTLN	291±18	142±14
C5-8	**HF**S**FL**F**S** PSFGVAGI FRFILFLQ GFHNWTLN	>400	139±17
C5-13	**VG**S**N**FF**G** PSFGVAGI FRFILFLQ GFHNWTLN	159±18	101± 5
C5-14	Q**N**S**LVL**A PSFGVAGI FRFILFLQ GFHNWTLN	126±14	100±10
C5-15	**G**SS**YY**F**G** PSFGVAGI FRFILFLQ GFHNWTLN	159± 8	113±20
C5-16	**HW**S**F**F**VS** PSFGVAGI FRFILFLQ GFHNWTLN	104±12	118±18
S6	QSSWFFA **MPL**G**IS**G**T** FRFILFLQ GFHNWTLN	130±27	130±17
C7-1	QSSWFFA PSFGVAGI F**G**F**VVRFL** GFHNWTLN	116±16	136±16
C7-2	QSSWFFA PSFGVAGI F**VY**I**VRIF** GFHNWTLN	215±15	93± 5
C7-3	QSSWFFA PSFGVAGI FR**WWF**F**VL** GFHNWTLN	140± 2	361±68
C7-5	QSSWFFA PSFGVAGI FRF**M**L**I**L**A** GFHNWTLN	136±13	124±12
S8	QSSWFFA PSFGVAGI FRFILFLQ **AE**HN**ILMH**	110±15	61± 5
C8-1	QSSWFFA PSFGVAGI FRFILFLQ G**A**H**AVLQL**	134±16	52± 4
C8-2	QSSWFFA PSFGVAGI FRFILFLQ **A**FH**GFIMQ**	142±22	46± 6
C8-4	QSSWFFA PSFGVAGI FRFILFLQ **S**FHN**FL**L**V**	145± 3	64+12
F188E	QSSWFFA PSFGVAGI FRFILFLQ G**E**HNWTLN	120+11	116±15
W191L	QSSWFFA PSFGVAGI FRFILFLQ GFHN**L**TLN	145±14	57± 6
T192A	QSSWFFA PSFGVAGI FRFILFLQ GFHNW**A**LN	115±18	98± 8

[a] This list includes combinatorial mutants (strain names starting with C), two mutants (S6 and S8) in which a D2 region was substituted with the corresponding region of D1, and several site-directed mutants. Mutated residues are bold. Data are the means ± the standard error determined from at least three replicates. [b] Photoautotrophic growth rates were measured in PS I-containing strains. The doubling time of the wild-type (WT) *Synechocystis* strain was 10.5 ± 1.0 h. [c] The half-time of F_V decay ($t_{1/2}$) was measured in PS I-less strains.

Fluorescence Decay. Some CD-loop D2 mutants are known to have modified charge recombination characteristics between the acceptor and donor sides of PS II (*16*). To investigate the effect of mutations in the CD-loop of D2 on charge recombination, the decay of the F_V yield after illumination for 100 ms was followed in intact PS I-less cells in the presence of DCMU. Under these conditions, the rate of Q_A^- reoxidation due to recombination of the negative charge with the donor side is monitored. The results for two combinatorial mutants (one with a slower and one with a faster rate of charge recombination in comparison with the control) are shown in Figure 1. The curves of the charge recombination kinetics in all mutants could be adequately fitted by two components with the rate constants of the fast

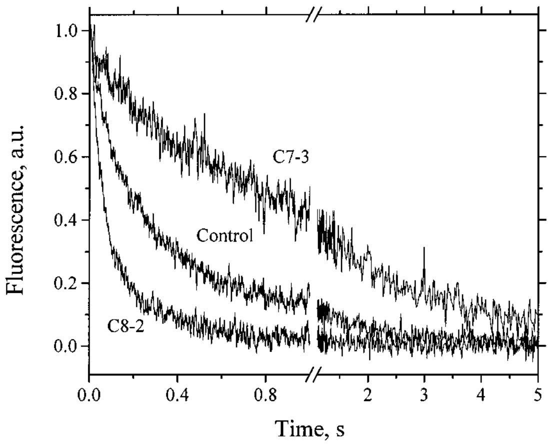

FIGURE 1: Decay of F_V in the control strain and in the C7-3 and C8-2 mutants in the presence of 10 μM DCMU. All three strains are in a PS I-less background. Variable fluorescence was induced by a 100 ms illumination of the cells with red light (100 μE m^{-2} s^{-1}) emitted by a PAM LED lamp. Each curve represents an average of four to six traces, and each trace was recorded using a fresh sample. Variable fluorescence has been normalized to be 1.0 at the end of the illumination period. The measuring light used to monitor fluorescence decay did not have a measurable actinic effect.

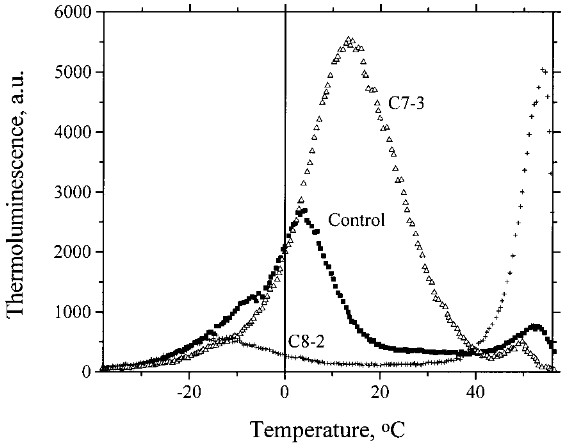

FIGURE 2: Representative TL curves measured in the control strain and the C7-3 and C8-2 mutants of *Synechocystis* sp. PCC 6803 in the presence of 50 μM DCMU. All three strains are in a PS I-less background. TL bands were excited by a train of 10 single-turnover flashes at −40 °C. The heating rate was 0.4 °C/s. Small differences in the chlorophyll concentration between the samples were corrected for.

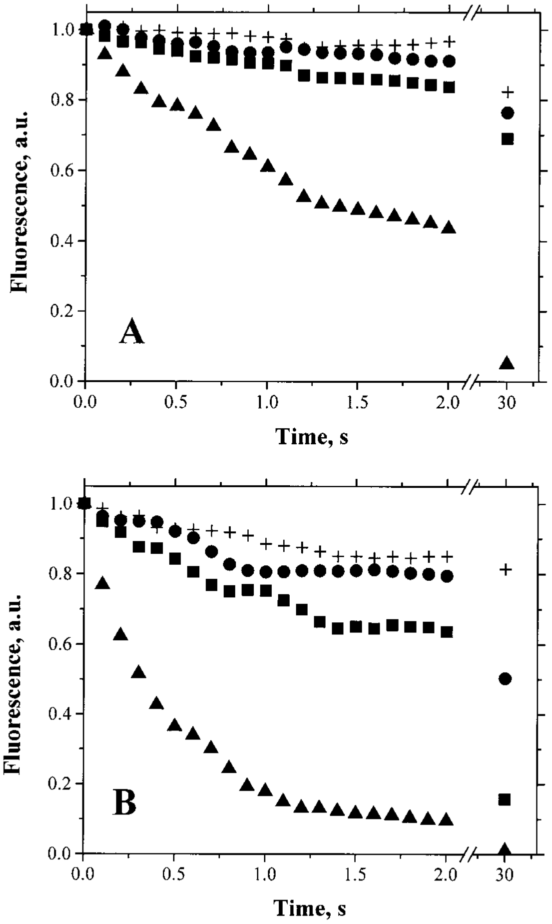

FIGURE 3: Temperature dependence of F_V decay measured in the control strain (A) and in the C8-2 mutant (B) treated with DCMU. Both strains are in a PS I-less background. Samples were incubated at −40 (+), −20 (●), −10 (■), or 0 °C (▲) and were illuminated with a 100 ms pulse of red PAM LED light (30 μE m^{-2} s^{-1}). Subsequently, the decay of F_V was monitored after termination of the pulse. Each curve represents a single, representative measurement.

and slow components ranging between 4 and 35 s^{-1} and between 0.5 and 5.3 s^{-1}, respectively. In the majority of mutants, both components decayed faster than in the control strain, whereas in the C7-3 mutant, the two components were noticeably slower than the control. Table 1 shows the overall decay half-times of variable fluorescence, $t_{1/2}$, in different CD-loop mutants. The overall half-time of F_V decay was taken to be an adequate parameter for Q_A^- stability for two reasons: (i) the fast and slow components of fluorescence decay changed nearly proportionally from mutant to mutant, and (ii) the intensity of each of the two phases was significant ($^1/_3$−$^2/_3$ of the overall intensity) and did not change greatly between the strains. In the absence of DCMU, Q_A^- oxidation rates in all mutants were similar to those in the wild type (not shown), thus indicating normal acceptor side properties.

Thermoluminescence Properties. Typical TL signals from different PS I-less strains of *Synechocystis* treated with DCMU and illuminated at −40 °C are presented in Figure 2. The control PS I-less strain exhibited an intense TL emission peak at ~4 °C, characteristic of a Q-band ($S_2Q_A^-$ recombination) with a small shoulder at approximately −10 °C. In addition, there was a second peak at ~50 °C (C-band), the origin of which remains controversial (see refs *25*−*27*).

In the C7-3 mutant, the Q-band of TL was much more pronounced and its maximum was shifted toward a higher temperature (13 °C) (Figure 2). In contrast, in the C8-2 strain, essentially no Q-band could be detected regardless of whether the cells were illuminated with a sequence of 10 single-turnover flashes (Figure 2) or continuously illuminated for 1 min at −40 °C (data not shown). However, the C8-2 mutant exhibited a large C-band at ~50 °C. Despite the inability to generate a Q-band in the C8-2 mutant, a stable charge-separated state appears to have been formed in this mutant after illumination at −40 °C. Exposure of DCMU-treated cells to either continuous illumination or flashes at −40 °C caused an increase in the fluorescence intensity due to formation of Q_A^-; at this temperature, the increased fluorescence yield exhibited a very slow decay in darkness at a rate similar to that in the control strain (Figure 3). At −40 °C, ~20% of the Q_A^- had disappeared after 30 s in both the control strain and the C8-2 mutant. However, the decay of variable fluorescence was accelerated markedly in the C8-2

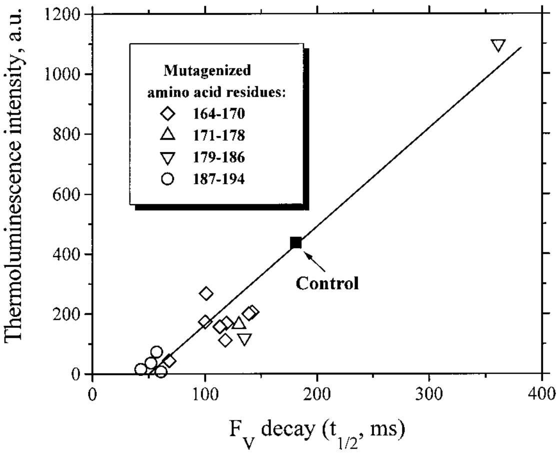

FIGURE 4: Correlation between the intensity of the Q-band of thermoluminescence and the half-time of fluorescence decay (with 10 μM DCMU) that were observed for different CD-loop mutants. The mutants and the control strain are in a PS I-less background. The TL signal was calculated as the integrated amount of emitted light that was detected over the temperature range from −30 to 40 °C and was normalized to the chlorophyll content in the sample. The decay of F_V was measured as indicated in the legend of Figure 1, and the decay half-time was plotted. Different symbols indicate different mutagenized regions of the CD-loop, as indicated in the inset.

mutant at −20 °C, whereas in the control strain, the decay rate of Q_A^- at −20 °C was almost as slow as that at −40 °C. At 0 °C, the decay half-time was ~0.5 and 2 s in the C8-2 and the control strains, respectively. Therefore, in the C8-2 mutant, charge recombination occurs without leading to TL emission.

The temperature behavior of F_V decay suggests that Q_A^- is largely reoxidized in the C8-2 and control strains during the course of the TL recording; the heating rate during the TL recording was 0.4 °C/s, and only a very small portion of the centers with Q_A^- remained after several seconds of darkness at 20 °C (Figure 1). Consequently, the origin of the large C-band in the C8-2 mutant is not easily explained. Either the electron on Q_A^- does not participate in charge recombination leading to TL emission at ~50 °C, or only a minor fraction of the PS II centers (those that retain Q_A^- at >45 °C) is responsible for the major C-band observed in the C8-2 mutant at 50 °C.

Other mutants with a rapid rate of charge recombination also exhibited a very large decrease in the intensity of the Q-band of TL, whereas as shown in Figures 2 and 3, the C7-3 mutant coupled a slow charge recombination rate with a large intensity of the Q-band of TL. In fact, this correlation appears to be general for the CD-loop mutants; the intensity of the Q-band (the TL signal integrated over the −30 to 40 °C temperature range) measured in different CD-loop mutants is proportional to $t_{1/2}$, the half-time of F_V decay in the presence of DCMU (Figure 4). It should be emphasized that the linear relationship between the Q-band intensity and $t_{1/2}$ in Figure 4 is drawn only to illustrate the general trend, and no specific proportionality between the intensity of the Q-band of TL and the charge recombination rate can be theoretically predicted at this point.

There is also a correlation between the position of T_M (the temperature maximum of the Q-band) and the half-time of F_V decay. As presented in Figure 2, the C7-3 mutant that has a slow F_V decay ($t_{1/2}$ ~ 360 ms) has a T_M of ~13 °C, whereas the control strain ($t_{1/2}$ ~ 180 ms) exhibited a T_M of ~4 °C, and in mutants with a $t_{1/2}$ of F_v decay ranging from 100 to 140 ms, T_M was decreased by 0−3 °C compared to that for the control strain. The C8-2 mutant and those similar to it with the fastest F_V decay ($t_{1/2}$ ~ 50 ms) had a small TL peak, which may represent recombination involving remaining Q_A^- with the donor side, at approximately −15 °C.

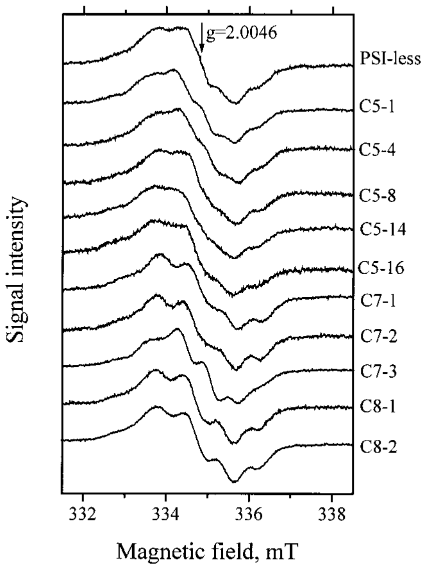

FIGURE 5: Comparison of the EPR spectra of the Tyr$_D^{ox}$ radical in thylakoid membranes of the PS I-less control strain and different combinatorial mutants in the PS I-less background. Experimental parameters were as follows: temperature, 120 K; microwave power, 1 mW; microwave frequency, 9.41 GHz; modulation amplitude, 0.3 mT; and modulation frequency, 100 kHz. The chlorophyll concentration in the samples was 200−270 μg/mL.

Y_D^{ox} EPR Properties. To determine whether combinatorial mutations in the CD-loop region affected the PS II conformation at the donor side, EPR spectra of Y_D^{ox} were recorded in thylakoids isolated from different PS I-less strains. All combinatorial mutants exhibited a dark-stable signal with a g value of ~2.004 (Figure 5), which resembled signal II$_s$ (g = 2.0046) in the control PS I-less strain; this signal originates from Y_D^{ox}. However, the fine structure of this signal in the mutants was modified in various ways depending on the mutations introduced into the CD-loop (Figure 5). These effects are rather minor and are smaller than when introducing single-site mutations involving residues interacting with Y_D (*16*, *28*, *29*). The amplitude of the Y_D^{ox} signal, normalized to the Chl *a* content in the corresponding thylakoid preparations, was similar in all samples, suggesting that the various mutants retained a dark-stable Y_D^{ox} and confirming that they have a similar amount of PS II centers on a Chl basis. Therefore, the properties of Y_D^{ox} were not affected greatly by the combinatorial mutations, suggesting that no major structural rearrangements have occurred in PS II as a function of the combinatorial changes that were introduced.

DISCUSSION

The data presented here show that mutations in the CD-loop region on the lumenal side of the D2 protein of PS II modify the lifetime of Q_A^- if electron transfer to Q_B is blocked by DCMU. Moreover, TL measurements done with a set of CD-loop mutants with altered charge recombination kinetics have revealed that the relative yield of the Q-band

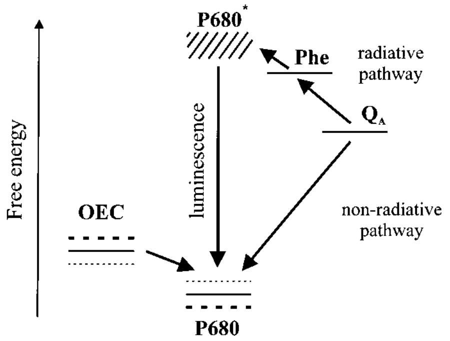

FIGURE 6: Schematic model for explaining the mutation-induced changes in the Q_A^- decay rate and the thermoluminescence yield. Changes in the prevalence of nonradiative vs radiative charge recombination are due to alteration of the equilibrium $\Delta G°$ between the $P680^+S_1$ and $P680S_2$ states. The energy levels for P680 and the S states of the Mn cluster of the oxygen-evolving complex in control PS II are indicated as solid lines. If the $\Delta G°$ between $P680^+S_1$ and $P680S_2$ becomes smaller [i.e., the P680 level increases or the S state level decreases (thin dashed lines)], the equilibrium concentration of $P680^+$ during the lifetime of the $S_2Q_A^-$ state will increase. At low temperatures (up to approximately −10 °C), only the nonradiative path is expected to contribute significantly to Q_A^- decay, thus depleting the level of the charge-separated state in PS II without leading to TL; at such temperatures, the radiative recombination reaction will be essentially “frozen”. However, in the C7-3 mutant, the $\Delta G°$ between $P680^+S_1$ and $P680S_2$ appears to have become larger [because either the S_2 level increases or the P680 level decreases (fat dotted lines)], thus decreasing the rate of the back reaction $P680S_2 \rightarrow P680^+S_1$ and the equilibrium concentration of $P680^+$. As a consequence, the charge recombination rate at low-temperature is reduced as compared to the control system, and more PS II with a charge-separated state is still present when a sample of this mutant is warmed. As charge recombination slows, the TL peak of this mutant shifts to higher temperatures.

of TL (due to $S_2Q_A^-$ state recombination) correlates strongly with the lifetime of Q_A^-. The recorded TL curves were normalized to the Chl content of the sample, which, in turn, in first approximation is proportional to the amount of PS II centers in PS I-less *Synechocystis* strains retaining a significant amount of PS II centers (*16*). All strains used in the experiments presented here were able to evolve oxygen at high rates; their PS II activity was high enough to support photoautotrophic growth in a PS I-containing background, and most of the mutants exhibited a normal oscillation pattern of O_2 evolution upon illumination with single-turnover flashes. The stable reduction of Q_A upon illumination at −40 °C and Q_A^- reoxidation upon warming of the samples were evident from fluorescence measurements (see Figure 3). Therefore, the large spread in the intensity of the Q-band between the different mutants reflects changes in the TL yield upon $S_2Q_A^-$ recombination rather than changes in the yield of formation of this state upon illumination or changes in the concentration of functional PS II centers (expressed on a chlorophyll basis).

A plausible working hypothesis for explaining the data presented in this paper is that there is a charge recombination pathway that does not lead to TL and that is enhanced in mutant strains with more rapid charge recombination. This hypothesis, which is schematically illustrated in Figure 6, will be discussed and expanded upon in the following paragraphs, after discussing mutational effects on the properties of the donor side of PS II.

Changes in Donor Side Equilibria. The first question to be discussed is what the functional relationship may be between the modified CD-loop sequence and the altered lifetime of Q_A^-. Experimental data and the results of homology-based structural modeling localize the CD-loop at the lumenal (donor) side of the thylakoid membrane, with some amino acid residues apparently in close contact with the accessory Chls associated with P680 (*16*, *17*, *30*, *31*). Therefore, the alterations in charge recombination kinetics are likely to be due to a modification at the donor side of PS II. However, it is known that severe impairment at the donor side can induce changes in the midpoint redox potential (E_m) of Q_A (*32*), which is ∼27 Å from $P680^+$ (*33*). We do not favor the possibility of functional alterations at the acceptor side causing the effects observed in our mutants because (i) the slightly modified form of the Y_D^{ox} EPR spectra observed in most of the strains that were tested (Figure 5) together with essentially unaltered oxygen evolution suggest a minor conformational change at the donor side of PS II as a function of the combinatorial mutations, (ii) electron transfer from Q_A to Q_B is essentially unaffected (data not shown), and (iii) if TL shifts to lower temperatures were due to a shift in the E_m of the Q_A/Q_A^- couple, this shift should not have caused a decrease in TL intensity.

The altered charge recombination kinetics observed in the mutants are best explained by a change in the energy gap between the $P680^+S_1$ and $P680S_2$ states, which shifts the equilibrium between P680 and the water-splitting apparatus. This is expected to affect charge recombination, the rate of which (among other factors) is determined by the steady state concentration of oxidized P680 during the lifetime of the charge separation between Q_A^- and the oxidized donor side (*34*). Mutants with a fast F_V decay are expected to have an equilibrium of the $P680^+S_1 \Leftrightarrow P680S_2$ reaction that is more to the left compared to the situation in the control strain that carries the wild-type CD-loop sequence. In contrast, the C7-3 mutant that is characterized by a slow F_V decay may have a $P680^+S_1 \Leftrightarrow P680S_2$ reaction equilibrium that is more to the right than in the control. The apparent change in the equilibrium between the $P680^+S_1$ and $P680S_2$ states can be due to a shift in the E_m of either the $P680^+/P680$ couple or the S_1/S_2 states of the oxygen-evolving complex. We prefer to attribute the change in equilibrium to a change in the $P680^+/P680$ E_m as the oxygen evolution properties remained unchanged for many of the mutants that have a high rate of charge recombination.

There are several examples of how the protein matrix of a photosynthetic pigment−protein complex can alter the E_m of redox active (bacterio)chlorophylls (*35*−*37*). For instance, addition or removal of one hydrogen bond to or from the bacteriochlorophyll dimer of the bacterial reaction center changed the E_m of the primary donor by 50−80 mV (*35*). Mutation of the presumed P700 ligand His656 to Asn or Ser in the PS I reaction center protein *psa*B increased the oxidation midpoint potential of the $P700/P700^+$ couple by 40 mV (*36*). On the basis of the results of site-directed mutagenesis (*16*), the electrostatic influence of Arg180 in the D2 protein has been estimated to elevate the oxidizing potential of the $P680-P680^+$ couple by ≈100 mV above the E_m value of a hydrogen-bonded Chl *a* (*38*). As residues in the CD-loop are likely to affect the interaction of this and other residues with P680, mutations in the CD-loop can indeed modify the hydrogen bonding and electrostatic interactions with P680, thereby altering its midpoint potential.

Recombination Pathways. An altered equilibrium of the $P680^+S_1 \Leftrightarrow P680S_2$ reaction in the CD-loop mutants explains the modified Q_A^- stability in the presence of DCMU, but this discussion has not yet addressed the question of how these alterations may affect the TL yield. The present view of photosynthetic TL (reviewed in ref *14*) suggests that separated charges at the donor and acceptor sides of PS II are reasonably stable at low temperatures and as the thermal energy increases upon warming the probability of forming the $P680^+Pheo^-$ radical pair is increased as well. The recombination of $P680^+Pheo^-$ can result in the formation of singlet excited P680* with subsequent light emission either from P680* or from the coupled antenna Chls. Besides this, a nonradiative path that involves electron transfer from Q_A^- to $P680^+$ has also been proposed (*10*, *12*).

The existence of two competing pathways of Q_A^- decay in PS II, one of which is radiative and leads to the formation of P680* and (thermo)luminescence emission and the second of which is nonradiative and therefore does not lead to the formation of P680* (Figure 6), provides a good explanation for the observed TL and fluorescence data. However, to understand the experimental observations (i.e., the absence of TL in C8-2 and other mutants), it is imperative that the nonradiative pathway exist at low temperatures (less than approximately −10 °C) and is augmented in the mutants that lack TL, whereas the radiative pathway is insignificant in this temperature range. This interpretation is very reasonable as the activation energy of the nonradiative recombination pathway is expected to be much smaller than that of the radiative pathway. To recombine radiatively, the $S_2Q_A^-$ state must be activated by an energy of more than 700 mV (the free energy difference between the $P680S_2$ and $P680^+S_1$ states, which is ~100 mV according to ref *39*, plus the free energy difference between the $P680^*Q_A$ and $P680^+Q_A^-$ states, which is nearly 600 mV according to ref *1*). The nonradiative charge recombination is likely not to involve the formation of a $P680^+Pheo^-$ charge pair, but rather a charge recombination between Q_A^- and $P680^+$ that leads to $P680Q_A$ formation. In this reaction, the only activation energy that is required is that of the formation of the $P680^+S_1$ state from the $P680S_2$ state ($\Delta G^\circ \sim 100$ mV in the wild type; significantly smaller in the mutants lacking TL). Therefore, our interpretation of the absence of the Q-band of TL in the C8-2 mutant and mutants similar to it is that the decrease in the energy gap between the $P680^+S_1$ and $P680S_2$ states facilitates nonradiative charge recombination at low temperatures. This depletes essentially all $S_2Q_A^-$ radical pairs during the TL recording before the rate constant of radiative recombination becomes high enough to observe TL.

Several possible pathways exist for nonradiative Q_A^- decay in PS II. These are direct electron transfer from Q_A^- to $P680^+$ (in view of its occurrence at low temperatures, involvement of Pheo is unlikely) and an indirect pathway of electron transfer involving cyt b_{559} or other intermediates. EPR measurements carried out with thylakoids isolated from different mutants used in this study have shown that cyt b_{559} is essentially in the oxidized low-potential form ($g = 2.93$) in samples that have been dark-adapted for a short period of time (data not shown). Therefore, cyt b_{559} in these samples may conceivably be reduced by the acceptor side. However, the nonradiative charge recombination pathway that is enhanced in the majority of mutants is not likely to involve cyt b_{559} for two reasons: (i) kinetic studies with different PS II preparations treated with DCMU have shown that reduced Q_A is a very inefficient reductant of cyt b_{559} (*8*, *40*), and (ii) treatment of cyanobacterial thylakoids with ascorbate, which can reduce cyt b_{559} (*41*), did not slow the decay of Q_A^-. Note that in these experiments we were not able to demonstrate the reduction of cyt b_{559} using EPR, since addition of ascorbate strongly modified the signal from the thylakoids at $g \approx 3$.

Nonradiative Pathway at Room Temperature. The data presented in this paper suggest that in the wild-type PS II centers a considerable amount of PS II charge separations has decayed via the nonradiative pathway before the temperature is high enough to allow the radiative charge recombination pathway. A determination of the relative importance of the radiative and nonradiative pathways under physiological conditions is less straightforward, and quantitative data for intact PS II to our knowledge have not been reported in the literature. The maximum TL shift in the C7-3 mutant from 5 to 13 °C is accompanied by a 2.5-fold increase in the amount of charge recombinations occurring via the radiative pathway. The time that elapses on heating from 5 to 13 °C (20 s; heating rate of 0.4 °C/s) in the C7-3 mutant is indicative of the lifetime of the charge-separated state of PS II in this mutant, and therefore, radiation-less decay occurs on a time scale of many seconds at this temperature. Judging from the relative temperature insensitivity of the nonradiative pathway (see ref *4*) and the increasing rate of recombination via the radiative pathway with increasing temperature, one can speculate that the radiative pathway at room temperature may be significant.

If so, this situation would be different than in bacterial reaction centers where the charge recombination between Q_A^- and the oxidized primary donor D^+ at room temperature was shown to occur almost exclusively by a nonradiative pathway (*42*). In DCMU-treated pea thylakoids with an inactive oxygen-evolving system, Jursinic and Govindjee (*43*) estimated that more than 90% of recombinations occur at room temperature via a nonradiative pathway, based on the comparison of the delayed luminescence and fluorescence (F_O) yields. However, in general a quantitative determination of this percentage from luminescence yield measurements is difficult for two reasons. In the first place, chlorophyll excitation resulting from charge recombination, which is likely to reside initially on P680, may be used more easily for charge separation than excitation absorbed by the antenna. Second, the F_O yield is likely to overestimate the probability of fluorescence and/or luminescence emitted by an open PS II, as at least in cyanobacteria this yield includes components with a long fluorescence lifetime that are not associated with the PS II complex (*44*) and a component associated with PS I.

In conclusion, the results of this study indicate that mutations in different areas of the CD-loop of the D2 protein modify the equilibrium between the $P680^+S_1$ and $P680S_2$ states, which in turn causes changes in charge recombination and TL characteristics of PS II. The results are also clearly indicative of a nonradiative recombination pathway, presumably involving direct recombination between Q_A^- and an oxidized chlorophyll associated with $P680^+$, which is the major recombination pathway at low temperatures and which also may be important in the wild-type PS II complex under physiological conditions.

ACKNOWLEDGMENT

We thank Dr. Jean-Marc Ducruet for the use of his thermoluminescence setup, for stimulating discussions, and for hospitality during D.V.V.'s stay at the Centre d'Études Nucléaires (Saclay, France). Dr. Svetlana Ermakova-Gerdes and Anna Keilty are acknowledged for the construction of the original combinatorial and replacement mutants, and Dr. Alain Boussac (CEN, Saclay, France) and Dr. Russell LoBrutto are thanked for their help with the flash-induced oxygen evolution measurements and with the EPR measurements, respectively. We thank Dr. Robert L. Burnap (Oklahoma State University, Stillwater, OK) for the measurement of the oscillation pattern of oxygen evolution in several mutants during preparation of the revised version of the manuscript.

REFERENCES

1. Diner, B. A., and Babcock, G. T. (1996) in *Oxygenic Photosynthesis: The Light Reactions* (Ort, D. R., and Yocum, C. F., Eds.) pp 213−247, Kluwer Academic Publishers, Dordrecht, The Netherlands.
2. Barber, J. (1998) *Biochim. Biophys. Acta 1365*, 269−277.
3. Buser, C. A., Thompson, L. K., Diner, B. A., and Brudvig, G. W. (1990) *Biochemistry 29*, 8977−8985.
4. Hillmann, B., and Schlodder, E. (1995) *Biochim. Biophys. Acta 1231*, 76−88.
5. Stewart, D. H., and Brudvig, G. W. (1998) *Biochim. Biophys. Acta 1367*, 63−87.
6. Thompson, L. K., and Brudvig, G. W. (1988) *Biochemistry 27*, 6653−6658.
7. Whitmarsh, J., and Cramer, W. A. (1977) *Biochim. Biophys. Acta 501*, 83−93.
8. Buser, C. A., Diner, B. A., and Brudvig, G. W. (1992) *Biochemistry 31*, 11449−11459.
9. Barber, J., and De Las Rivas, J. (1993) *Proc. Natl. Acad. Sci. U.S.A. 90*, 10942−10946.
10. Prasil, O., Kolber, Z., Berry, J. A., and Falkowski, P. G. (1996) *Photosynth. Res. 48*, 395−410.
11. Shopes, R. J., and Wraight, C. A. (1987) *Biochim. Biophys. Acta 893*, 409−425.
12. Krieger-Liszkay, A., and Rutherford, A. W. (1998) *Biochemistry 37*, 17339−17344.
13. Jursinic, P. A. (1986) in *Light Emission by Plants and Bacteria* (Govindjee, Amesz, J., and Fork, D. C., Eds.) pp 291−328, Academic Press, Orlando, FL.
14. Vass, I., and Govindjee (1996) *Photosynth. Res. 48*, 117−126.
15. Campbell, K. A., Peloquin, J. M., Diner, B. A., Tang, X.-S., Chisholm, D. A., and Britt, R. D. (1997) *J. Am. Chem. Soc. 119*, 4787−4788.
16. Manna, P., LoBrutto, R., Eijckelhoff, C., Dekker, J. P., and Vermaas, W. (1998) *Eur. J. Biochem. 251*, 142−154.
17. Xiong, J., Subramaniam, S., and Govindjee (1996) *Protein Sci. 5*, 2054−2073.
18. Ermakova-Gerdes, S., Vavilin, D., Keilty, A., and Vermaas, W. (1998) in *Photosynthesis: Mechanisms and Effects* (Garab, G., Ed.) Vol. IV, pp 2859−2864, Kluwer Academic Publishers, Dordrecht, The Netherlands.
19. Keilty, A. T., Ermakova-Gerdes, S. Y., and Vermaas, W. F. J. (2000) *J. Bacteriol. 182*, 2453−2460.
20. Rippka, R., Deruelles, J., Waterbury, J. B., Herdman, M., and Stanier, R. Y. (1979) *J. Gen. Microbiol. 111*, 1−61.
21. Vermaas, W. F. J., Charité, J., and Shen, G. (1990) *Biochemistry 29*, 5325−5332.
22. Ermakova-Gerdes, S., Shestakov, S., and Vermaas, W. (1995) in *Photosynthesis: from Light to Biosphere* (Mathis, P., Ed.) Vol. I, pp 483−486, Kluwer Academic Publishers, Dordrecht, The Netherlands.
23. Vavilin, D. V., Ermakova-Gerdes, S. Y., Keilty, A. T., and Vermaas, W. F. J. (1999) *Biochemistry 38*, 14690−14696.
24. Ducruet, J.-M., and Miranda, T. (1992) *Photosynth. Res. 33*, 15−27.
25. Ono, T., and Inoue, Y. (1989) *Biochim. Biophys. Acta 973*, 443−449.
26. Krieger, A., Weis, E., and Demeter, S. (1993) *Biochim. Biophys. Acta 1144*, 411−418.
27. Johnson, G. N., Boussac, A., and Rutherford, A. W. (1994) *Biochim. Biophys. Acta 1184*, 85−92.
28. Tang, X. S., Chisholm, D. A., Dismukes, G. C., Brudvig, G. W., and Diner, B. A. (1993) *Biochemistry 32*, 13742−13748.
29. Tommos, C., Davidsson, L., Svensson, B., Madsen, C., Vermaas, W., and Styring, S. (1993) *Biochemistry 32*, 5436−5441.
30. Svensson, B., Etchebest, C., Tuffery, P., van Kan, P., Smith, J., and Styring, S. (1996) *Biochemistry 35*, 14486−14502.
31. Xiong, J., Subramaniam, S., and Govindjee (1998) *Photosynth. Res. 56*, 229−254.
32. Johnson, G. N., Rutherford, A. W., and Krieger, A. (1995) *Biochim. Biophys. Acta 1229*, 202−207.
33. Hara, H., Dzuba, S. A., Kawamori, A., Akabori, K., Tomo, T., Satoh, K., Iwaki, M., and Itoh, S. (1997) *Biochim. Biophys. Acta 1322*, 77−85.
34. Chu, H. A., Nguyen, A. P., and Debus, R. J. (1995) *Biochemistry 34*, 5839−5858.
35. Lin, X., Murchison, H. A., Nagarajan, V., Parson, W. W., Allen, J. P., and Williams, J. C. (1994) *Proc. Natl. Acad. Sci. U.S.A. 91*, 10265−10269.
36. Webber, A. N., Su, H., Bingham, S. E., Kass, H., Krabben, L., Kuhn, M., Jordan, R., Schlodder, E., and Lubitz, W. (1996) *Biochemistry 35*, 12857−12863.
37. Merry, S. A. P., Nixon, P., Barter, L. M. C., Schilstra, M., Porter, G., Barber, J., Durrant, J. R., and Klug, D. R. (1998) *Biochemistry 37*, 17439−17447.
38. Mulkidjanian, A. Y. (1999) *Biochim. Biophys. Acta 1410*, 1−6.
39. Renger, G., Christen, G., Karge, M., Eckert, H.-J., and Irrgang, K.-D. (1998) *J. Biol. Inorg. Chem. 3*, 360−366.
40. Samson, G., and Fork, D. C. (1991) *Photosynth. Res. 27*, 179−187.
41. Thomson, L. K., Miller, A. F., Buser, C. A., de Paula, J. C., and Brudvig, G. W. (1989) *Biochemistry 28*, 8048−8056.
42. Woodbury, N. W., Parson, W. W., Gunner, M. R., Prince, R. C., and Dutton, P. L. (1986) *Biochim. Biophys. Acta 851*, 6−22.
43. Jursinic, P., and Govindjee (1982) *Photosynth. Res. 3*, 161−177.
44. Bittersmann, E., and Vermaas, W. (1991) *Biochim. Biophys. Acta 1098*, 105−116.

BI001679M